A Study on Symbol Timing Recovery Schemes for Broadband in-Home PLC

Javier Godoy[1], Francisco J. Cañete[2], José A. Cortés, Luis Díez
Departamento de Ingeniería de Comunicaciones
E.T.S.I. de Telecomunicación, University of Málaga, Spain
Email: [1]javier.godoy85@gmail.com, [2]francis@ic.uma.es

***Abstract*—In this paper, algorithms for synchronization acquisition on multi-carrier transmission systems for broadband in-home power-line communications (PLC) are analyzed. Three symbol synchronization methods are studied and compared over realistic PLC channel models. These algorithms are evaluated as part of a PLC system that includes practical techniques for channel estimation, equalization and bit loading and whose parameters are set according to PLC standards.**

I. Introduction

In the last years, PLC communications are getting more and more attention for many applications [1], local area networks at homes and small offices being one of them. The development of efficient broadband systems and, recently, the release of two international standards: ITU G.hn [2] and IEEE 1901 [3], is remarkable. In smart-grids applications, PLC is playing an important role as well. Utilities have been using this technology since long time and new standards are expected in the near future, like ITU G.hnem and IEEE 1901.2 for narrowband systems. This paper is focused on broadband indoor PLC where multi-carrier modulation is agreed as the best technique to cope with channels characteristics. The common case in current PLC standards is to use packet-oriented transmission and a crucial task is the correct packet detection and symbol timing estimation. For this purpose, the packets have a structure of a starting header plus the payload. The header contains preambles for packet detection, synchronization and channel estimation. The packet lengths are short enough to disregard sampling time correction in synchronization and just symbol timing is adjusted.

In several previous works, the problem of symbol timing estimation in OFDM (Orthogonal Frequency Division Multiplexing) systems has been addressed. In some of them [4], from a more theoretical perspective, in others [5][6], from a more practical one or in [7], covering both aspects. However, the design of the proposed algorithms was made for wireless systems and tests were carried out over AWGN (Additive White Gaussian Noise) channels or wireless channel models, but few results for PLC have been published so far. PLC channels exhibit unique characteristics that prevent the direct implementation of techniques designed for other contexts. It is worth mentioning the high frequency selectivity and the time variation of the channel response [8] or the relevance of impulsive noise [9]. An interesting proposal can be found in [10], focused on narrowband PLC systems and with solutions tested on a simple two-tap multipath channel. In this work, some synchronization schemes are studied, modified and applied to PLC systems. To this end, multi-carrier modulation parameters extracted from broadband PLC standards and realistic PLC channel models, taken from [11] and [12], are employed to estimate the algorithms performance by means of simulations. The objective is to evaluate simple and practical transmission techniques useful in the development of experimental PLC systems or prototypes, since, usually, the solutions in commercial high performance modems are proprietary.

In the next section, the transmission system is described, including some of the involved signal processing algorithms. In the third section, the proposed synchronization protocol and methods for timing estimation are addressed and, in the fourth one, these schemes are tested over PLC channels models. Finally, some conclusions are given in the last section.

II. System description

The proposed system follows a classical multi-carrier DMT (discrete multi-tone) scheme based on the FFT (fast Fourier transform) algorithm. It is essentially the same as an OFDM implementation but without analogue carrier. The modulating signal is created directly in baseband and hence the whole broadband signal is synthesized in discrete-time, and it is real valued. The DMT symbol (*symbol* here after) length is $N_{cp} + N$ samples in the time domain, where N_{cp} samples are the cyclic prefix and subsequent N samples contain the useful information. The cyclic prefix (CP), or guard interval, is inserted in the transmitted signal and removed before demodulating at reception. The system can be approximated as $N/2$ parallel independent and flat sub-channels, provided that the CP is longer than the effective length of the channel impulse response. Once set N_{cp}, the higher the number of sub-channels, the more efficient the system. The information to transmit is mapped into M-QAM (or BPSK) modulated data for each of the carriers and the modulation is implemented by means of an IFFT (inverse FFT) of the M-QAM symbols (that represent complex samples in the frequency domain). At the IFFT output, the CP samples are obtained and added to the time domain samples of the DMT modulated signal.

Since HomePlug is one of the most successful commercial standards for in-home PLC modems, the proposed multi-carrier system parameters are adapted to HomePlug 1.0 and

Table I
SYSTEM PARAMETERS

parameter	HomePlug 1.0	HomePlug AV
frequency band	0-25 MHz	0-37.5MHz
sampling freq.	50 MHz	75 MHz
FFT points, N	256	3072
available carriers	128	1536
useful carriers	84	1155
useful band	4.49-20.7 MHz	1.8-30 MHz
CP samples, N_{cp}	172	372+{417,567,3534}
symbol length(μs)	8.56	{51.48,53.48,139.56}
Modulations	B/DB/DQ-PSK	B-PSK,M-QAM*
max bit rate	14 Mb/s	200 Mb/s

*$M \in \{4, 16, 64, 256, 1024\}$

HomePlug AV, which are summarized in Table I. The modulation is BPSK for all carriers in header symbols but, depending on the selected standard, it can be variable in the remaining symbols.

The data to transmit is previously organized in packets composed by a header and the payload. The header has been defined as a preamble in the form of seven known symbols. At reception, the time domain samples must be firstly synchronized, but this part is explained in detail in the next section. Hence, assuming that synchronization has been acquired, the following are the functions to correctly receive the information data.

Firstly, the CP samples are discarded and the remaining N samples are the input to an FFT that acts as demodulator to get the complex M-QAM data of each carrier. Let $B_{m,k}$ denote one of these for the m-th received symbol at the carrier of frequency index k:

$$B_{m,k} = A_{m,k} \cdot H_k + Z_{m,k}. \tag{1}$$

where H_k is the channel response, $A_{m,k}$ the transmitted modulated data on that carrier and $Z_{m,k}$ the noise component, sampled at the receiver at that frequency.

A. Channel estimation

In Homeplug 1.0 differential modulation is employed, therefore no channel equalization is required at reception and no channel estimation needed. On the contrary, for Homeplug AV simulations a simple channel estimation procedure is proposed. It employs five subsequents identical symbols in the preamble (after the two first symbols for synchronization).

The algorithm is based on a *maximum likelihood* estimator that calculates the mean of $B_{m,k}$ that is

$$\frac{1}{P}\sum_{m=1}^{P} B_{m,k} = A_k \cdot H_k + \frac{1}{P}\sum_{m=1}^{P} Z_{m,k}. \tag{2}$$

Since the transmitted modulated data is the same over P DMT symbols ($P = 5$ in this case) and the channel is supposed invariant during the P symbols, the estimation is obtained as:

$$\hat{H}_k = \frac{1}{A_k}\left(\frac{1}{P}\sum_{m=1}^{P} B_{m,k} - \frac{1}{P}\sum_{m=1}^{P} Z_{m,k}\right). \tag{3}$$

The noise sum tends to zero in case of zero-mean random noise and the estimator approaches

$$\hat{H}_k \simeq \frac{1}{A_k}\left(\frac{1}{P}\sum_{m=1}^{P} B_{m,k}\right). \tag{4}$$

B. Frequency Equalization

One of the main advantages of multi-carrier modulation is the straight-forward method for channel equalization. In a well designed system a single coefficient can be used at each sub-channel in the form of the so-called frequency equalizer (FEQ). In this work, the coefficient is estimated according to a *zero-forcing* criterion (non-optimal but simple) to compensate for the estimated channel frequency response:

$$FEQ_k = \frac{1}{\hat{H}_k}, \tag{5}$$

and the equalized data at each carrier is

$$\hat{A}_{m,k} = FEQ_k \cdot B_{m,k} = \frac{1}{\hat{H}_k} \cdot B_{m,k}, \tag{6}$$

which approximates the transmitted data and constitutes the input to the decision block corresponding to the constellation of each carrier.

C. Bit-loading

In multi-carrier modulation, since the broadband channel is decomposed in $N/2$ sub-channels, the transmitted signal on each carrier can be adapted to the particular sub-channel conditions. In this work, a *bit-loading* technique is employed that assigns a different constellation size on each carrier according to its estimated signal to noise conditions, denoted as SNR_k. The technique consists in an optimization process in which the goal is to maximize the bit-rate achieved by the system under the restriction of an available power at the transmitter and a certain mean bit error probability (P_B) at the receiver. The optimal solution to this problem in Gaussian noise channels is well known, the so-called *water-filling* approach that consists in allocating denser constellations at the carriers with more SNR_k.

The following equation provides an estimation of the number of bits per symbol (b_k) to put in the constellation assigned to carrier k,

$$b_k = \left\lfloor \log_2\left(1 + \frac{SNR_k}{\Gamma_k}\right)\right\rfloor. \tag{7}$$

Where $\lfloor x \rfloor$ denotes the integer part, because an integer number of bits is assigned to each constellation. Additionally, only square M-QAM modulations are assumed (with Gray code mapping). The latter restriction leads to include an *SNR gap*, denoted as Γ_k, which models the losses in the achievable rate due to the use of a practical modulation scheme. The *SNR gap* is defined according to a target P_B (in AWGN) by using the inverse of the Q-function,

$$\Gamma_k = \frac{1}{3}\left[Q^{-1}\left(\frac{P_b}{4}\, b_k\right)\right]^2, \tag{8}$$

what leads to an implicit equation in b_k that can be solved with some practical approximations [13], to obtain

$$\Gamma_k = -\frac{1}{1.6}\ln\left(\frac{P_b}{0.2}\right). \quad (9)$$

III. Synchronization protocol

A symbol synchronization protocol with the initial functions of the receiver has been designed. It is performed over the two first symbols in the preamble [1], i.e. before channel estimation, and includes packet detection, automatic gain control (AGC) and symbol timing estimation.

A. Packet detection and AGC

The first element at the receiver is an estimator of instantaneous energy to detect that signal is arriving. It employs an envelope detector over squares of the incoming samples and consists in a sliding window averaging algorithm with a window of a symbol length. Then, the estimated energy is compared to an heuristic threshold to trigger the packet detection when preamble appears. A normalization on the estimated energy is performed to obtain a gain coefficient that serves as AGC. In this way, the detected packet amplitude in set among predictable levels for the timing estimation algorithm. A time correction is also carried out to compensate for the delay introduced by the envelope detector, with a safety margin, to guarantee that the timing estimation starts inside the CP samples of the first symbol in header.

B. Symbol timing estimation

For the symbol synchronization, three methods are considered and compared. The goal is to identify some points of the header structure, in particular of the two initial symbols, to synchronize the packet reception.

1) Correlation Method: The first proposal is based on an intuitive criterion of maximum correlation. It exploits the fact that the cyclic prefix is a copy of the last samples of the symbol and tries to locate the maximum correlation sample.

A sliding window correlator of L samples computes the correlation between two windows separated N samples as shown in Fig. 1. The correlation metric is calculated as

$$P_1(n) = \sum_{m=0}^{L-1} r(n+m)\cdot r(n+m+N), \quad (10)$$

$r(n)$ being the received signal. In the absence of noise and distortion, maximums of $P_1(n)$ will appear at the first sample of a symbol. It is convenient to normalize that correlation metric to prevent strong fluctuations along the symbols due to the high peak-to-average power ratio (PAPR) that multi-carrier

[1]The system behavior is sensitive to the selection of symbols in the preamble with good autocorrelation properties. In this work, such symbols are obtained by simulation: minimizing P_B for the implemented algorithms. This preamble outperforms others obtained by the constellation scrambler proposed in [2].

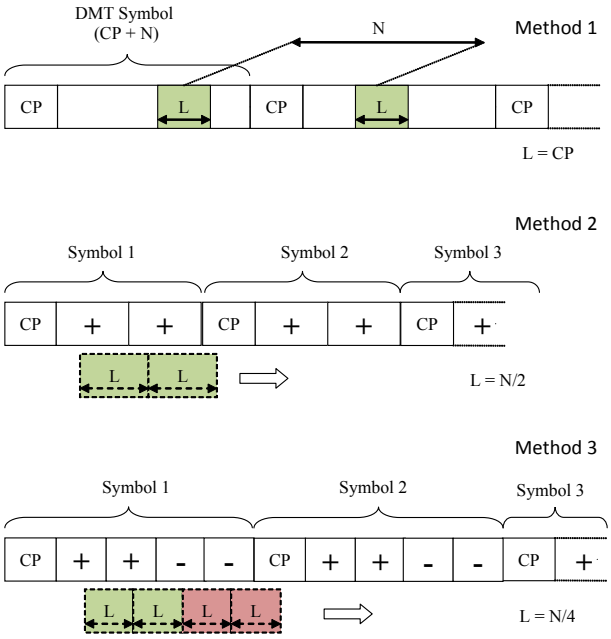

Figure 1. Header structure for the three timing estimation methods.

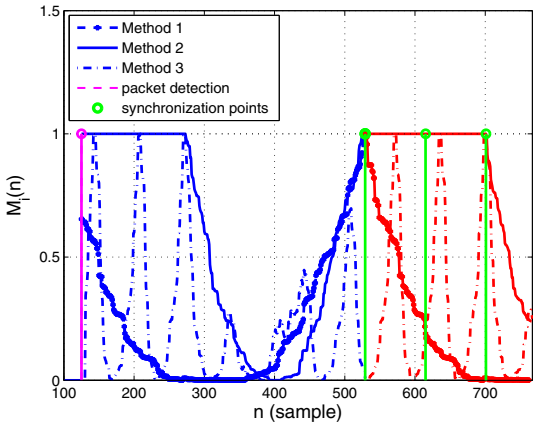

Figure 2. Timing metric for the three timing estimation methods. Homeplug 1.0 parameters are used. Blue line represents the length of the first symbol in header and red line corresponds to the second symbol.

signals usually exhibit. Hence, let $R_1(n)$ denote the estimation of the instantaneous energy contained in a L-length window[2],

$$R_1(n) = \sum_{m=0}^{L-1} |r(n+m+N)|^2. \quad (11)$$

Following the expressions taken from [5][6] for the next two methods, a common timing metric $M_i(n)$ with values between 0 and 1 is defined as:

$$M_i(n) = \frac{|P_i(n)|^2}{R_i^2(n)}. \quad (12)$$

The subscript will stand for the ordinal of the method, i.e. $M_1(n)$ in this case. In Fig. 2, an example of the $M_1(n)$

[2]In fact, the estimation performed in the AGC could be employed for this.

metric is shown when receiving a packet under ideal conditions (without noise and distortion). The correct synchronization sample is $\hat{n} = argmax\{M_1(n)\}$, located at the first sample of the second header symbol.

To get a better estimate, samples of both L-length windows can be computed in the energy normalization (although this increases the number of operations), what would lead to a new timing metric in which the term from (11) changes to

$$R_1'(n) = \frac{1}{2} \sum_{k=0}^{1} \sum_{m=0}^{L-1} |r(n+m+kN)|^2 . \quad (13)$$

2) Schmidl & Cox Method: This method was presented in [5] for OFDM signals. It uses a header symbol composed by two identical parts of $N/2$ samples and uses this redundancy to identify the beginning of the second symbol, see Fig. 1. The correlation metric is calculated between two consecutive windows of length $L = N/2$, i.e.

$$P_2(n) = \sum_{m=0}^{L-1} r(n+m) \cdot r(n+m+L) \quad (14)$$

Now $R_2(n)$ is the energy estimated in the L-length window involved in the correlation

$$R_2(n) = \sum_{m=0}^{L-1} |r(n+m+L)|^2 , \quad (15)$$

or it can be calculated in a double-length window, as mentioned above,

$$R_2'(n) = \frac{1}{2} \sum_{m=0}^{2L-1} |r(n+m)|^2 . \quad (16)$$

The use of the timing metric given by (12) leads to $M_2(n)$, which is shown in Fig. 2, as well for ideal conditions. It has a flat plateau whose center is located $L/2$ samples after the second symbol beginning and that can be estimated from the average sample between the two points at 90% of the maximum value. As it will be demonstrated, for more realistic noise and distortion conditions this method is not very accurate.

3) Minn & Bhargava Method: This algorithm is an evolution of the previous one and was presented in [6] for OFDM signals as well. Now the symbols in the preamble are divided into four identical parts of $L = N/4$ samples, the two last with an inverted polarity (see Fig. 1). The estimation is based on two correlations of L-length windows each: the first one between the two first consecutive windows, and the second one between the two last consecutive windows. Then both correlations are added to get the final correlation metric

$$P_3(n) = \sum_{k=0}^{1} \sum_{m=0}^{L-1} r(n+m+2kL) \cdot r(n+m+L+2kL). \quad (17)$$

Let $R_3(n)$ be the estimated energy for two of the L-length windows involved in the correlation

$$R_3(n) = \sum_{k=0}^{1} \sum_{m=0}^{L-1} |r(n+m+L+2kL)|^2 , \quad (18)$$

and, again, it can be calculated in a double-length window

$$R_3'(n) = \frac{1}{2} \sum_{m=0}^{4L-1} |r(n+m)|^2 . \quad (19)$$

The timing metric given by (12) allows to obtain $M_3(n)$, which is plotted in Fig. 2, under ideal conditions. The particularities in this metric makes it have three maximums per symbol. The sample of the last maximum is located to estimate the beginning of the second header symbol. While the others two synchronization methods do not present relevant changes in their metrics whether the parameters are selected according to HomePlug 1.0 or HomePlug AV, $M_3(n)$ does. Only two maximums per symbol appear when using the shortest CP in the HomePlug AV standard. In such a case, the last maximum must be located as well to get the symbol synchronization.

Metrics modification: The metrics in [5][6] were defined for OFDM, and so they process complex values corresponding to the low-pass equivalent signals. However, when using DMT the timing metrics can be simplified since the involved signals are real and the modulus operation is not needed, leading to

$$M_i(n) = \frac{|P_i(n)|^2}{R_i^2(n)} \quad \longrightarrow \quad M_i(n) = \frac{P_i(n)}{R_i(n)}. \quad (20)$$

In this way, metric values are not positive but $\in [-1, 1]$, although methods 1 and 2 behave essentially as explained above. Nevertheless, for method 3, some differences appear: $M_3(n)$ has two maximums and one minimum per symbol for HomePlug 1.0 parameters and one maximum and one minimum per symbol for HomePlug AV, hence it even simplifies the algorithm. The methods performances with the new timing metric is nearly the same, but with lower computational effort, for example the number of operations is reduced in more than one thousand for HomePlug 1.0 (see final values in table II).

There exists a more efficient implementation of these metrics that consists in using recursive formulas, for instance (10) can be calculated by means of

$$P_1(n+1) = P_1(n) + r(n+L) \cdot r(n+N+L) - r(n)r(n+N), \quad (21)$$

and (11) by means of

$$R_1(n+1) = R_1(n) + |r(n+N+L)|^2 - |r(n+N)|^2 \quad (22)$$

In any case, the first L samples must be calculated with the original equation and then the recursion is applied.

Methods comparison: In order to compare the three methods performance, their behavior over an AWGN channel is studied and their computational complexity in terms of the number of operations (*nop*) is evaluated. In Fig. 3, the mean and variance of the estimated synchronization samples are plotted. The estimated points are referred to the correct beginning of second header symbol. Simulations were carried out for 10^4 packet transmissions for different SNR values and using HomePlug 1.0 parameters. As shown, the mean value for methods 1 and 3 approaches the correct value for SNR over

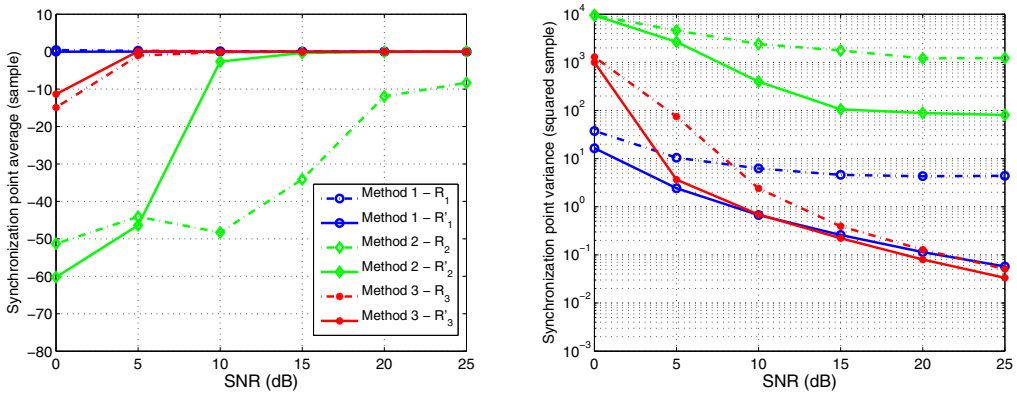

(a) mean of the estimated sample

(b) variance of the estimated sample

Figure 3. Timing metrics comparison in AWGN channels.

5dB, whereas method 2 only reaches that using $R'_2(n)$ and for SNR over 15 dB. Moreover, a lower variance is obtained for methods 1 (using $R'_1(n)$) and 3. As it can be expected, timing metrics with R'_i that employs more samples to normalize the energy gets better results.

Table II
NUMBER OF OPERATIONS OF THE TIMING METRICS

method	correlation	Schmidl&Cox	Minn&Bhargava
L	N_{cp}	N/2	N/4
sums (s)	T(3L-2)	T(3L-2)	T(6L-2)
products (p)	T(3L+2)	T(3L+2)	T(6L+2)
nop HP1.0	330ks+332kp	245ks+248kp	245ks+248kp
nop HPAV	13.7Ms+13.7Mp	26.7Ms+26.7Mp	26.7Ms+26.7Mp
nop HP1.0*	3078s+3723p	2946s+3591p	2946s+3591p

* recursive implem.

In Table II, the estimated *nop*, per synchronization attemp, for the timing metrics in the three methods are summarized[3]. The calculations are made for an interval of $T = 1.5(N_{cp}+N)$ total samples, one and a half symbol after the packet detection, what is enough for synchronization. Method 1 requires more *nop* for HomePlug 1.0 but lower for HomePlugAV, depending on the ratio between N_{cp} and N. Although Method 2 requires the same *nop* than Method 3, its behavior is worse, so it is discarded for evaluation over PLC channels. Note that the recursive implementation saves almost two orders of magnitude in *nop*.

IV. TESTS OVER REALISTIC PLC CHANNELS

In order to test the system behavior in more realistic conditions, the channel model proposed in [11] for indoor PLC channels is used. A diagram of the channel for the tests is shown in Fig.4. Different scenarios of channels response, background noise and impulsive noise are obtained from the channel generator and noise registers available at [12].

[3]For HP1.0: T=642, N_{cp}=172, N=256; for HPAV: T=5791, N_{cp}=789, N=3072 (samples).

In particular, there are three suggested channel responses corresponding to a best, medium and bad cases (where goodness indicates lower delay spread and attenuation). There are also three background noise power spectral density (PSD), estimated from measurements and denoted as heavily, medium and weakly disturbed cases. There are waveforms of typical impulsive periodic noise synchronous and asynchronous with the mains frequency of 50Hz (in Europe) (more details on impulsive noise can be found in [9]). In this work, the selected scenario is the combination of the worst channel and the highly disturbed background noise, with and without impulsive noise.

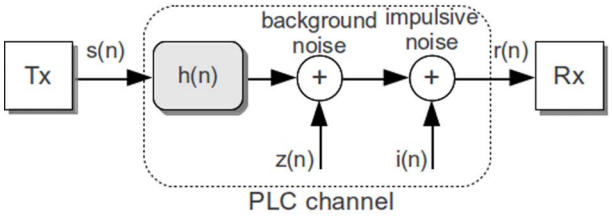

Figure 4. Diagram of the tests over PLC channels.

In the tests, 10^3 packets are transmitted with a payload that contains one hundred random data symbols (i.e. 10^5 DMT symbols). In PLC, for electromagnetic compatibility reasons, there are regulations that define masks to limit the maximum PSD at transmission. Hence, according to practical PLC systems, a flat PSD of -50 dBm/Hz and a target P_B of 10^{-3} are adopted here. The results of the analysis are: detection error, number of packets detected out of the CP of first header symbol; detection offset, mean difference between the estimated detection point and the ideal one (in number of samples); synchronization offset, mean difference between the estimated synchronization point and the ideal one (in number of samples); P_B, the measured value (that must be under the target one) and R_B, the achieved bit-rate. A small detection offset that does not lead to detection error is afterwards compensated by the synchronization algorithm or by the FEQ.

Table III
RESULTS OVER PLC CHANNELS

	HP1.0		HPAV		HP1.0 + imp.	
	met.1	met.3	met.1	met.3	met.1	met.3
det.error	0	0	0	0	0	0
det.offset	117	132	153	282	80.7	5.8
sync.offset	49	47	64	63	57	31
P_B	<min	<min	$1.8.10^{-5}$	$1.2.10^{-5}$	0.009	0.002
R_B (Mb/s)	18.34	18.34	41.94	41.94	18.34	18.34

In Table III, some simulations results are compiled for both standard parameters and also including impulsive noise for HP1.0 (for HPAV results are very similar). It can be observed that, in all cases, both synchronization methods reach similar results without detection errors in any packet, although Method 3 usually provides lower offsets and a P_B slightly better [4].

Simulations with HomePlug AV parameters for synchronization method 3, including bit-loading have been carried out as well. It must be mentioned that, in the simulated system, an ideal return channel is assumed and hence the transmitter knows the estimated channel to make the bit allocation. In these tests, the SNDR (signal to noise and distortion ratio) has been estimated at reception (before decision) to replace the SNR in (7), because with non-perfect synchronization and channel estimation, some ISI and ICI appear [5]. Otherwise, the bit load obtained (targeting an AWGN channel) would be overestimated for the actual PLC channels and the system P_B would be severely increased. In Fig.5, the received SNR and estimated SNDR (signal to noise and distortion rate) per carrier is plotted together with the allocated bits per symbol. The achieved bit rate in this case is 140Mb/s. Finally, in Fig.6, the actual P_B at each carrier for that simulation is shown and it complies with the target value in all cases.

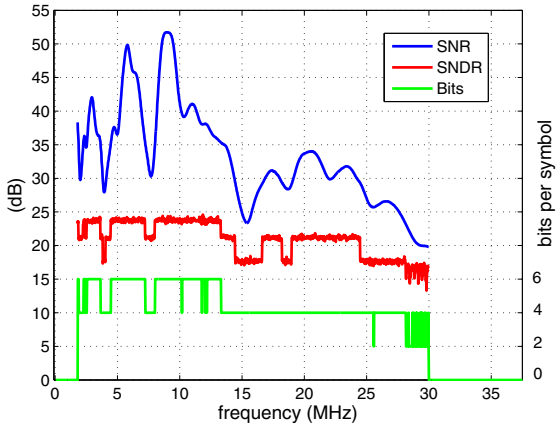

Figure 5. Bit-loading results in transmissions with HomePlug AV parameters (worst channel response and highly disturbed noise scenario).

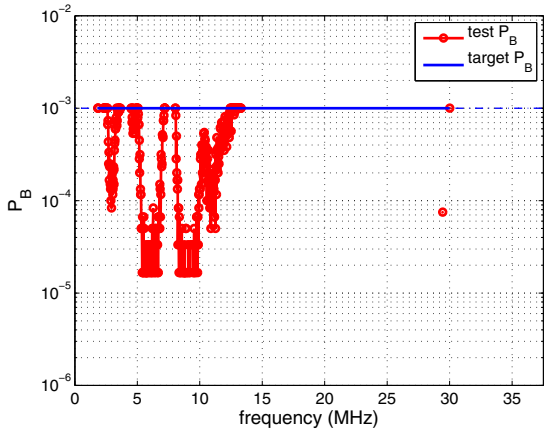

Figure 6. Bit error probability at each carrier for simulations in Fig.5. At carriers in the central band, the P_B is under the test floor (aprox. 10^{-5} for BPSK and 10^{-6} for 1024-QAM).

V. CONCLUSION

In this work, a multi-carrier system has been designed, according to current PLC standards parameters, to simulate some synchronization schemes under practical conditions. Three timing estimation algorithms have been analyzed and realistic indoor PLC channel models have been employed to evaluate the system performance.

REFERENCES

[1] Ferreira, H.; Lampe, L.; Newbury, J.; Swart, T. (Eds.) *Power Line Communications*, Wiley, 2010.

[2] "Unified high-speed wire-line based home networking transceivers – System architecture and physical layer specification," ITU-T Rec. G.9960, Jun 2010.

[3] "Broadband Over Power Line Networks: Medium Access Control and Physical Layer Specifications," IEEE Standard 1901, Sep 2010.

[4] Muller-Weinfurtner, S.H. "On the optimality of metrics for coarse frame synchronization in OFDM: a comparison," in *Proc. IEEE Int. Symp. on Personal, Indoor and Mobile Radio Comm.*, pp.533-537 vol.2, 1998.

[4] In HP1.0, DQPSK is used and the minimum P_B that could be measured is $6 \cdot 10^{-8}$, whereas in HPAV, QPSK is used and $4 \cdot 10^{-9}$ is the min. P_B.

[5] In addition, N_{cp} is taken from standards but channels from realistic models. Hence, the channel discrete-time response could be longer than CP.

[5] Schmidl, T.M.; Cox, D.C. "Robust frequency and timing synchronization for OFDM," *IEEE Trans. on Communications*, pp.1613-1621, Dec 1997.

[6] Minn, H.; Bhargava, V.K. "A simple and efficient timing offset estimation for OFDM systems," in *Proc. Vehicular Technology Conference* VTC 2000-Spring Tokyo, pp.51-55 vol.1, 2000.

[7] Seol, C.; Cheun. K. "Maximum-Likelihood Symbol Timing Estimation Algorithm for OFDM Systems Based on a Repeated Preamble," in *Proc. Asia-Pacific Conf. on Communications*, pp.1-5, Aug 2006.

[8] Cañete, F.J.; Cortés, J.A.; Díez, L.; Entrambasaguas, J.T. "Analysis of the cyclic short-term variation of indoor power-line channels," *IEEE Journal on Selected Areas in Communications*, Jul 2006, pp.1327-1338.

[9] Cortés, J.A.; Díez, L.; Cañete, F.J.; Sánchez-Martínez, J.J. "Analysis of the Indoor Broadband Power-Line Noise Scenario," *IEEE Transactions on Electromagnetic Compatibility*, Nov 2010, pp.849-858.

[10] Bumiller, G.; Lampe, L. "Fast Burst Synchronization for Power Line Communication Systems," EURASIP Journal on Advances in Signal Processing 2007.

[11] Cañete, F.J.; Cortés, J.A.; Díez, L.; Entrambasaguas, J.T. "A Channel Model Proposal for Indoor Power Line Communications," *IEEE Communications Magazine*, pp.166-174, Dec 2011.

[12] *PLC channel generator*. PLC Group - Ing. Comunicaciones Dpt., Universidad de Málaga. [Online] http://www.plc.uma.es

[13] Chung, S.T.; Goldsmith, A.J. "Degrees of freedom in adaptive modulation: A unified view," *IEEE Trans. on Communications*, pp. 1561-1571, Sep 2001.